Received: 26 March 2021 | Revised: 1 May 2021 | Accepted: 3 May 2021

DOI: 10.1002/jcla.23853

RESEARCH ARTICLE

WILEY

MiR-133a-3p attenuates resistance of non-small cell lung cancer cells to gefitinib by targeting SPAG5

Qing Li[1] | Yueming Wang[2] | Jingdong He[1]

[1]Clinical Laboratory of Tianjin Chest Hospital, Tianjin, China

[2]School of Stomatology, Tianjin Medical University, Tianjin, China

Correspondence
Qing Li, Clinical Laboratory of Tianjin Chest Hospital, Tianjin, China
Email: lqyt6688@163.com

Abstract

Background: Gefitinib is an epidermal growth factor receptor tyrosine kinase inhibitor (EGFR-TKI), clinically used to treat patients with non-small cell lung cancer driven by EGFR mutations. Unfortunately, EGFR-TKI resistance has become a clinical problem for the effective treatment of NSCLC patients. The purpose of this study was to explore the effect and mechanism of miR-133a-3p on the gefitinib sensitivity of NSCLC cells.

Methods: The gefitinib-resistant PC9 (PC9/GR) cells were established through repeated long-term exposure to gefitinib for half a year. Then, PC9/GR cells were transfected with miR-133a-3p mimics and PC9 cells were transfected with miR-133a-3p inhibitors to increase or decrease the expression of miR-133a-3p. CCK-8 assay, colony formation assay, and caspase-3 activity assay were employed to detect cell resistance to gefitinib. Quantitative real-time PCR and Western blotting were used to evaluate the levels of miR-133a-3p, SPAG5, and other related genes. Starbase database was used to predict the target gene of miR-133a-3p and the prognosis of NSCLC patients. Target gene of miR-133a-3p was verified through dual-luciferase reporter gene assay.

Results: MiR-133a-3p was significantly downregulated in gefitinib-resistant cell line PC9/GR vs. gefitinib-sensitive cell line PC9. Overexpression of miR-133a-3p increased the sensitivity of NSCLC cells to gefitinib and vice versa. Furthermore, SPAG5 is an important target gene of miR-133a-3p, and SPAG5 can reverse miR-133a-3p-mediated gefitinib sensitivity of NSCLC cells.

Conclusions: These findings indicated that miR-133a-3p/SPAG5 axis played a vital role in acquired resistance to gefitinib in NSCLC cells, and miR-133a-3p may represent a potential therapeutic strategy for the treatment of human NSCLC.

KEYWORDS
gefitinib resistance, miR-133a-3p, NSCLC, signaling pathway, SPAG5

1 | INTRODUCTION

Non-small cell lung cancer (NSCLC), the most important subtype of lung cancer, is the leading cause of cancer deaths worldwide.[1] Clinically, compared with traditional therapies such as radiotherapy and chemotherapy, epidermal growth factor receptor tyrosine kinase inhibitors (EGFR-TKIs) are currently the first choice for NSCLC driven by EGFR mutations. Gefitinib, the most common

Qing Li and Yueming Wang These authors contributed equally for the work.

EGFR-TKIs, is often used as a first-line anti-tumor drug of advanced NSCLC with EGFR mutations.[2,3] However, 6 months or a year after gefitinib is used, the tumor will develop drug resistance, which seriously reduces the therapeutic effect of NSCLC patients.[4] Therefore, there is an urgent need to solve the difficult problem of gefitinib resistance.

MicroRNAs (miRNAs) are many small non-coding RNAs that downregulate target gene expression by binding to the 3'-untranslated region (3'-UTR) of mRNAs.[5] Lots of studies have indicated that microRNA plays a crucial role in diverse pathological processes, including oncogenesis and drug resistance such as gefitinib.[6-8] It has been reported that miR-133a-3p plays a tumor suppressor function in many cancers, including lung cancer, hepatocellular carcinoma, breast cancer, and esophageal squamous cell carcinoma.[9-12] Many studies have shown that miR-133a-3p is also a key regulator of drug resistance. For example, miR-133a-3p could increase the sensitivity to cisplatin via targeting ATP7B gene in Hep-2v cells.[13] MiR-133a-3p overexpression could enhance the sensitivity to doxorubicin by inhibiting the expression of mitochondria uncoupling protein 2 (UCP-2) in doxorubicin-resistant breast cancer cells.[14] However, the regulatory role of miR-133a-3p on gefitinib sensitivity in cancer is still unclear.

Sperm-associated antigen 5 (SPAG5) has been shown to regulate the timing of spindle organization and sister chromatid separation through binding to microtubules.[15,16] Currently, growing evidence has demonstrated that SPAG5 is closely related to tumorigenesis and had an oncogenic role.[17] Increased SPAG5 expression promoted the malignant progression and indicated a poor prognosis in lung cancer, breast cancer, prostate cancer, and hepatocellular carcinoma.[18-21] And SPAG5 has also been shown to be closely associated with chemoresistance in breast cancer and cervical cancer.[22,23] These studies clearly show that SPAG5 is a carcinogenic driver gene and may be a potential therapeutic target for cancer treatment.

In this study, we first established the gefitinib-resistant cell lines (PC9/GR) from PC9 cells by gradually increasing gefitinib exposure. Then, the influence of miR-133a-3p on the sensitivity of PC9 and PC9GR cells to gefitinib and its molecular mechanism is explored. Our results may suggest a potential treatment strategy to overcome gefitinib resistance by targeting miR-133a-3p.

2 | MATERIALS AND METHODS

2.1 | Bioinformatics analysis

RNA seq data of NSCLC patients obtained from The Cancer Genome Atlas (TCGA) database and Gene Expression Omnibus (GEO)/GSE48414 data set were used to explore the expression of miR-133a-3p and SPAG5 in NSCLC tissues and normal adjacent tissues. In this study, Starbase database [24] was used to predict the target gene of miR-133a-3p and the prognosis of NSCLC patients.

2.2 | Cell culture

The NSCLC cell line PC9 was obtained from the American Type Culture Collection. Gefitinib-resistance PC9 (PC9/GR) cell line was produced through repeated long-term exposure to gefitinib.[25,26] Briefly, PC9 cells were cultured and exposed with 0.2 μmol/L of gefitinib for 48h. Then, cells were cultured in the drug-free medium until cell fusion of about 80%. Then, cells were re-exposed with a higher concentration of gefitinib. When the cells could grow in gefitinib (5 μmol/L), PC9/GR cells were identified. All cell lines were cultured in RPMI-1640 containing 10% fetal bovine serum (FBS) at 37 C with 5% CO_2.

2.3 | CCK-8 assay

Cell Counting Kit-8 (CCK-8; Signal way Antibody LLC) assay was used to evaluate cell proliferation according to the manufacture's protocol. Cells were plated in 96-well plates at the density of 5×10^3 cells for 24 h at 37°C. Then, we exposed the cells to different concentrations of gefitinib. After incubation for 48 h, we added 20 μl of CCK-8 solution to each well and incubated at 37°C 5% CO_2 for 2 h. Then, we use a microplate reader to measure absorbance at an optical density of 450 nm.

2.4 | Colony formation assay

After transfection for 48 h, cells were added into 6-well plates (300 cells/well) and cultured in RPMI-1640 medium for 12 h. Then, cells were incubated in the medium with or without gefitinib for 48 h. After replaced medium with the gefitinib-free medium for 12 days of culture, we fixed the cells with methanol for 10 min and stained them with 1% crystal violet for 25 min. Finally, photography was performed and cell colonies formed by more than 50 cells indicated 1 clone.

2.5 | Caspase-3 activity assay

Following transfection for 48 h, cells were incubated in the medium with or without gefitinib for 48 h. Then, the activity of caspase-3 was detected in cells using the Caspase-3 Assay kit (Sigma-Aldrich, Merck KGaA) according to the manufacturers' instructions.

2.6 | Reverse transcription-quantitative PCR (RT-qPCR)

Total RNA was extracted from the cultured cells using TRIzol® reagent according to the manufacturer's protocol. MiR-133a-3p was quantified using TaqMan® MicroRNA Assays. RT-qPCR was performed using SYBR Green (Takara) with primers:

miR-133a-3p forward, 5′-GCCTTTGGTCCCCTTCAAC-3′, miR-133a-3p reverse, 5′-TATGCTTGTTCTCGTCTCTGTGTC-3′, SPAG5 forward, 5′-CATCTCACAGTGGGATAACTAATAAAC-3′, SPAG5 reveres 5′- CAGGGAT AGGTGAAGCAAGGATA-3′, U6 forward, 5′-CTCGCTTCGGCAGCACACA-3′, U6 reverse, 5′-AACGCTTCACGAATTTGCGT-3′, β-actin forward, 5′-TGGCACCCAGCACAATGAA-3′, β-actin reverse 5′-CTAAGTCA TAGTCCGCCTAGAAGCA-3′. Relative gene expression levels were calculated using the $2^{-\Delta\Delta Ct}$ method with β-actin or U6 snRNA as internal controls.

2.7 | Cell transfection

miR-133a-3p mimics (5′-UUUGGUCCCCUUCAACCAGCUG-3′), negative mimics control (5′- UUCUCCGAACGUGUCACGUTT-3′), miR-133a-3p inhibitor (5′-CAGCUGGUUGAAGGGGACCAAA-3′), negative inhibitor control (5′-CAGUACUUUUGUGUAGUACAA-3′), siRNA-SPAG5 and siRNA negative control, pcDNA3.1-SPAG5 and pcDNA3.1-Vector plasmids were synthesized by Ribobio. PC9/GR and PC9 cells were seeded in 6-well plates (1×10^6 cells/well). Lipofectamine 2000 Reagent was used for the transfection. The medium was replaced 6h after transfection. 100 nmol/L miR-133a-3p mimics, miR-133a-3p inhibitor, and siRNA-SPAG5 or 1.6 μg of pcDNA3.1-SPAG5 / Vector plasmids were used for cell transfection, and the expression levels of miR-133a-3p and SPAG5 were quantified after 48 h.

2.8 | Western blotting

Cells were lysis in RIPA lysis buffer for 30 min on ice. The lysate was cleared by centrifugation at 1000 rpm for 10 min, and the total protein concentration of the supernatant was measured by BCA protein assay. 5% non-fat milk was used to block the membranes for 1 h. Then the membranes were cultured overnight with primary antibodies against SPAG5 (1:500, #HPA022008, Sigma-Aldrich), PI3K (1:1500, #MA1-74183, Invitrogen), p-PI3K (1:1000, #PA5-99367, Invitrogen), AKT (1:2000, #2920, Cell Signaling Technology), p-AKT (1:1000, #44-621G, Invitrogen), GAPDH (1:5000, #5174, Cell Signaling Technology). After washing with PBS supplemented with Tween 20 for 3 times (8 min/time), the membranes were incubated with a horseradish peroxidase-conjugated goat anti-rabbit secondary antibody (1:4000, #ab6721, Abcam) for 1 h. Protein bands visualized using an Enhanced Chemiluminescence (ECL, Abcam) reagent. Protein expression levels were analyzed using the ImageJ software.

2.9 | Dual-luciferase reporter assay

Cells were seeded into 24-well plates for 24 h, and then co-transfected with 100 ng of luciferase reporter plasmid PGL3-WT-SPAG5/PGL3-MUT-SPAG5 (Shanghai, GenePharma), and 100 nmol/L of miR-133a-3p mimics or mimics negative control and miR-133a-3p inhibitors or inhibitor negative control. After 48 h, luciferase activities were measured with a Dual-Luciferase Reporter Assay System (Promega).

2.10 | Statistical analysis

Statistical analysis was performed using GraphPad 5.0 software (USA). The Student's t test was chosen to measure the difference between two groups and one-way ANOVA followed by Bonferroni post hoc test was used to measure differences among three groups. $p < 0.05$ was considered a statistically significant difference. The values are displayed in the form of mean ± standard deviation (SD).

3 | RESULTS

3.1 | Establishment of gefitinib-resistant PC9 (PC9/GR) cell lines

The gefitinib-resistant PC9/GR cell lines were established in increasing concentrations of gefitinib by the above method for half a year. The sensitivity of PC9 and PC9/GR cells to gefitinib was detected via CCK-8 assay and colony formation assay. The results revealed that PC9 cells were much more sensitive to gefitinib compared with PC9/GR (Figure 1A-C). Further, we checked the expression level of miR-133a-3p in PC9 and PC9/GR cells via RT-PCR and found that the expression level of miR-133a-3p in PC9/GR cells was markedly lower than PC9 cells (Figure 1D).

3.2 | Low expression of miR-133a-3p is significantly correlated with a poor prognosis in patients with lung cancer

We further explored the expression of miR-133a-3p in NSCLC. By analyzing GEO/GSE48414 data and TCGA/LUAD (Lung adenocarcinoma) data, we found that miR-133a-3p expression was lower in NSCLC tissues compared with normal lung tissues (Figure 2A-B). Notably, the survival analysis of NSCLC patients in the Starbase showed that low expression of miR-133a-3p was significantly correlated with a poor prognosis in NSCLC patients (Figure 2C).

3.3 | Upregulation of miR-133a-3p expression reverses gefitinib resistance in PC9/GR cells

Since miR-133a-3p was downregulated in PC9/GR cells versus PC9 cells, we hypothesized that miR-133a-3p expression level was associated with gefitinib sensitivity. To confirm whether upregulation of miR-133a-3p expression increased gefitinib sensitivity in NSCLC cells, we first transfected miR-133a-3p mimic in PC9/GR cells and

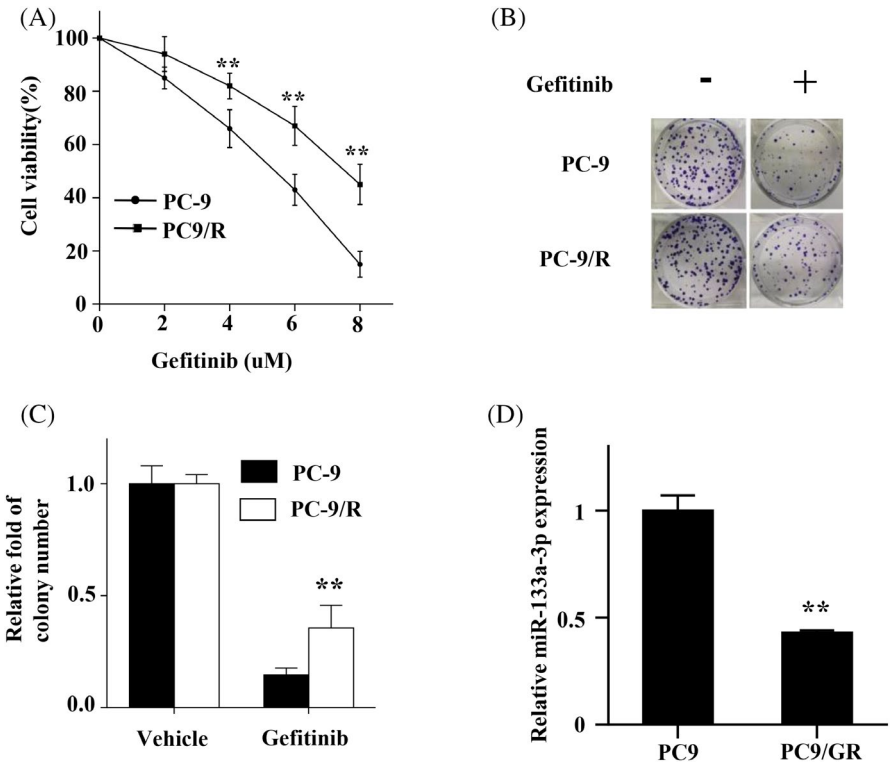

FIGURE 1 Gefitinib-resistant PC9 (PC9/GR) cell lines were established. (A) Proliferation of PC9 and PC9/GR cells treated with various concentrations of gefitinib was determined by CCK8 assay. (B-C) Colony-forming capability of PC9 and PC9/GR cells treated with gefitinib. (D) The expression of miR-133a-3p in PC9 and PC9/GR cells.

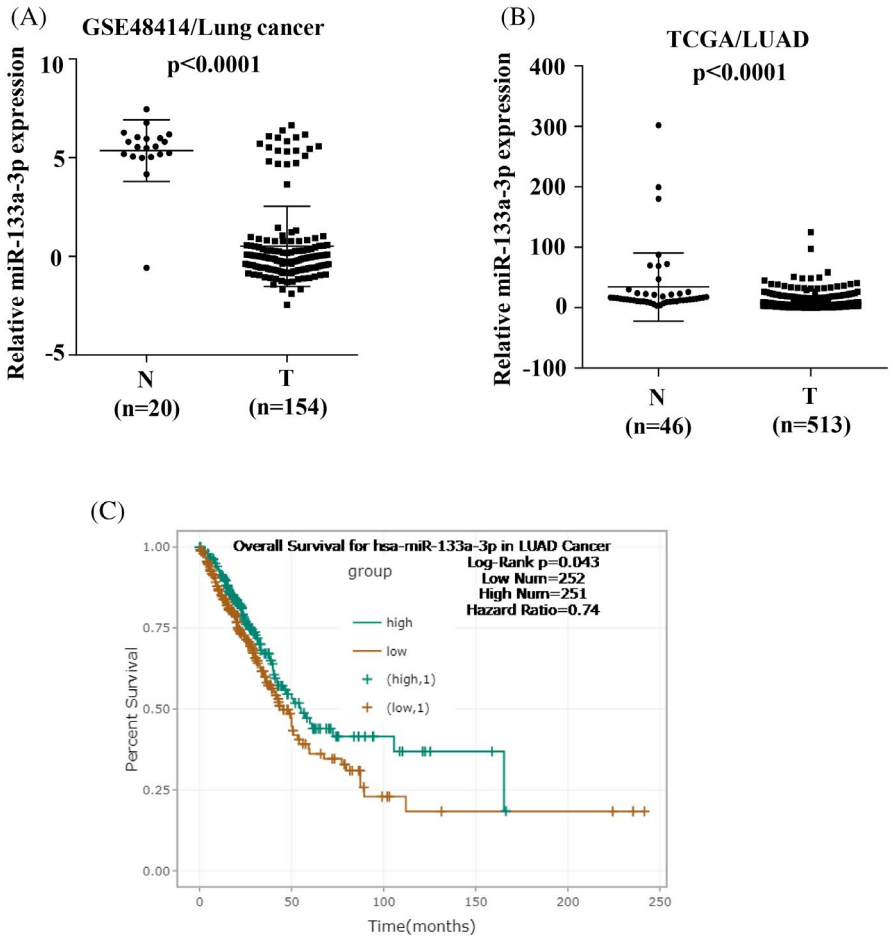

FIGURE 2 Low expression of miR-133a-3p is significantly correlated with a poor prognosis in NSCLC patients. Comparison of miR-133a-3p expression between NSCLC samples and normal lung tissues using data obtained from the (A) GEO/GSE48414 dataset and (B) TCGA database. (C) Kaplan-Meier OS analysis of LUAD patients downloaded from Startbase database.

examined the response of PC9/GR cells to gefitinib. As shown in Figure 3A, the expression of miR-133a-3p was significantly upregulated in the PC9/GR cells transfected with miR-133a-3p mimics compared to the control group cells. Then, the CCK-8 assay detecting the cell viability showed a significant reduction in viability of miR-133a-3p mimic cells after treated with different concentrations of gefitinib compared to mimic control cells (Figure 3B). We further explored the colony-forming capability of PC9/GR cells transfected with miR-133a-3p mimics upon to the gefitinib. The results showed that the colony-forming capability of the overexpression miR-133a-3p group was inhibited significantly when compared to the negative control group (Figure 3C-D). Besides, to clarify whether upregulation miR-133a-3p induced apoptosis of PC9/G cells, a caspase-3 activity assay was performed to detect changes in caspase-3 activity after gefitinib treatment. As shown in Figure 3E, under gefitinib exposure, the caspase-3 activity of PC9/GR cells transfected with miR-133a-3p mimic was significantly increased compared to PC9/GR cells transfected with the mimics control. Consistently, we found the expression of the pro-apoptotic protein Bax was increased and that of the anti-apoptotic Bcl-2 was decreased in PC9/GR cells upregulating miR-133A-3p compared with control cells after gefitinib treatment (Figure 2F). These findings suggested that upregulation miR-133a-3p induced apoptosis of PC9/G cells upon gefitinib. Taken together, the above results indicated that overexpression of miR-133a-3p could markedly increase the sensitivity of the PC9/GR cells to gefitinib.

To confirmed the results, we also transfected miR-133a-3p inhibitors in PC9 cells (Figure 3G) and repeated the above experiments. The downregulation of miR-133a-3p in PC9 cells promoted cell proliferation (Figure 3H-J) and decreased cell apoptosis (Figure 3K-L) upon gefitinib treatment. Taken together, these results indicated that miR-133a-3p plays a critical role in the gefitinib sensitivity of NSCLC cells.

3.4 | MiR-133a-3p suppresses PI3K/AKT pathway in PC9/GR cell line

PI3K/AKT signal pathway has been shown to play an important role in the gefitinib resistance of NSCLC cells.[32] To determine if PI3K / AKT signal mediates the regulation of gefitinib sensitivity by miR-133a-3p, we measured the protein expression of phosphorylated PI3K, total PI3K, phosphorylated AKT, total AKT by western blot analysis. We observed that the expression level of p-PI3K and p-AKT were markedly decreased by transfected with miR-133a-3p mimics in PC9/GR cells, while the total PI3K and AKT had no significant difference in expression (Figure 4A). Simultaneously, the expressions of p-PI3K and p-AKT protein in PC9- miR-133a-3p inhibitor cells were much higher than control cells (Figure 4B). These data suggested that miR-133a-3p may suppress PI3K/AKT signaling to increase the sensitivity of NSCLC cells to gefitinib.

3.5 | SPAG5 is a direct target of miR-133a-3p

In general, miRNAs perform their functions by suppressing the expression of downstream target genes. We predicted target genes of miR-133a-3p using the Starbase database and selected SPAG5 as a potential candidate target gene (Figure 5A). First, we analyzed the expressions of SPAG5 in LUAD patients by analyzing the TCGA database. The data showed a marked increase in SPAG5 expression was observed in NSCLC patient tissues (Figure 5B). Furthermore, the expression correlation between miR-133a-3p and SPAG5 was evaluated with Spearman's correlation analysis. The result showed that SPAG5 expression was negatively correlated with miR-133a-3p expression (Figure 5C). In addition, through Starbase database analysis, we found that high expression of SPAG5 was significantly associated with poor prognosis of NSCLC patients (Figure 5D). These results suggested that SPAG5 may be a potential target of miR-133a-3p in NSCLC.

To further validate whether miR-133a-3p can directly bind to the SPAG5 3'-UTR, we performed a dual-luciferase reporter assay. As shown in Figure 5E, the luciferase activity was significantly decreased in PC9/GR cells co-transfected with miR-133a-3p mimics and WT-SPAG5 compared with the control group, whereas no change was found in PC9/GR cells co-transfected with miR-133a-3p mimics and MUT-BIRC5. Meanwhile, the luciferase activity was significantly increased in PC9 cells co-transfected with miR-133a-3p inhibitors and WT-SPAG5 compared with the control group (Figure 5F). We next investigated whether miR-133a-3p regulated SPAG5 expression via check the mRNA and protein expression of SPAG5. The results revealed that overexpression of miR-133a-3p markedly repressed the expression of SPAG5 in PC9/GR cells (Figure 5G-H). Similarly, SPAG5 expression was significantly increased after transfected miR-133a-3p inhibitors in PC9 cells (Figure 5I-J). Overall, these data demonstrated that SPAG5 is a direct target of miR-133a-3p.

FIGURE 3 Upregulation of miR-133a-3p expression reverses gefitinib resistance in PC9/GR cells. (A) The expression of miR-133a-3p in the PC9/GR cells transfected with miR-133a-3p mimics or mimics control. (B) Proliferation of PC9/GR cells transfected with miR-133a-3p mimics or mimics control after treated with various concentrations of gefitinib was determined by CCK8 assay. (C-D) Colony-forming capability of PC9/GR cells transfected with miR-133a-3p mimics or mimics control after treated with gefitinib. (E) Caspase-3 activity was detected in cells exposed to gefitinib. (F) Protein expression of Bax, Bcl-2, and GAPDH in PC9/GR cells was determined by western blotting. (G) The expression of miR-133a-3p in the PC9 cells transfected with miR-133a-3p inhibitor or inhibitor control. (H) Proliferation of PC9 cells transfected with miR-133a-3p inhibitor or inhibitor control after treated with various concentrations of gefitinib was determined by CCK8 assay. (I-J) Colony-forming capability of PC9 cells transfected with miR-133a-3p inhibitor or inhibitor control after treated with gefitinib. (K) Caspase-3 activity was detected in cells exposed to gefitinib. (L) Protein expression of Bax, Bcl-2, and GAPDH in PC9 cells was determined by western blotting.

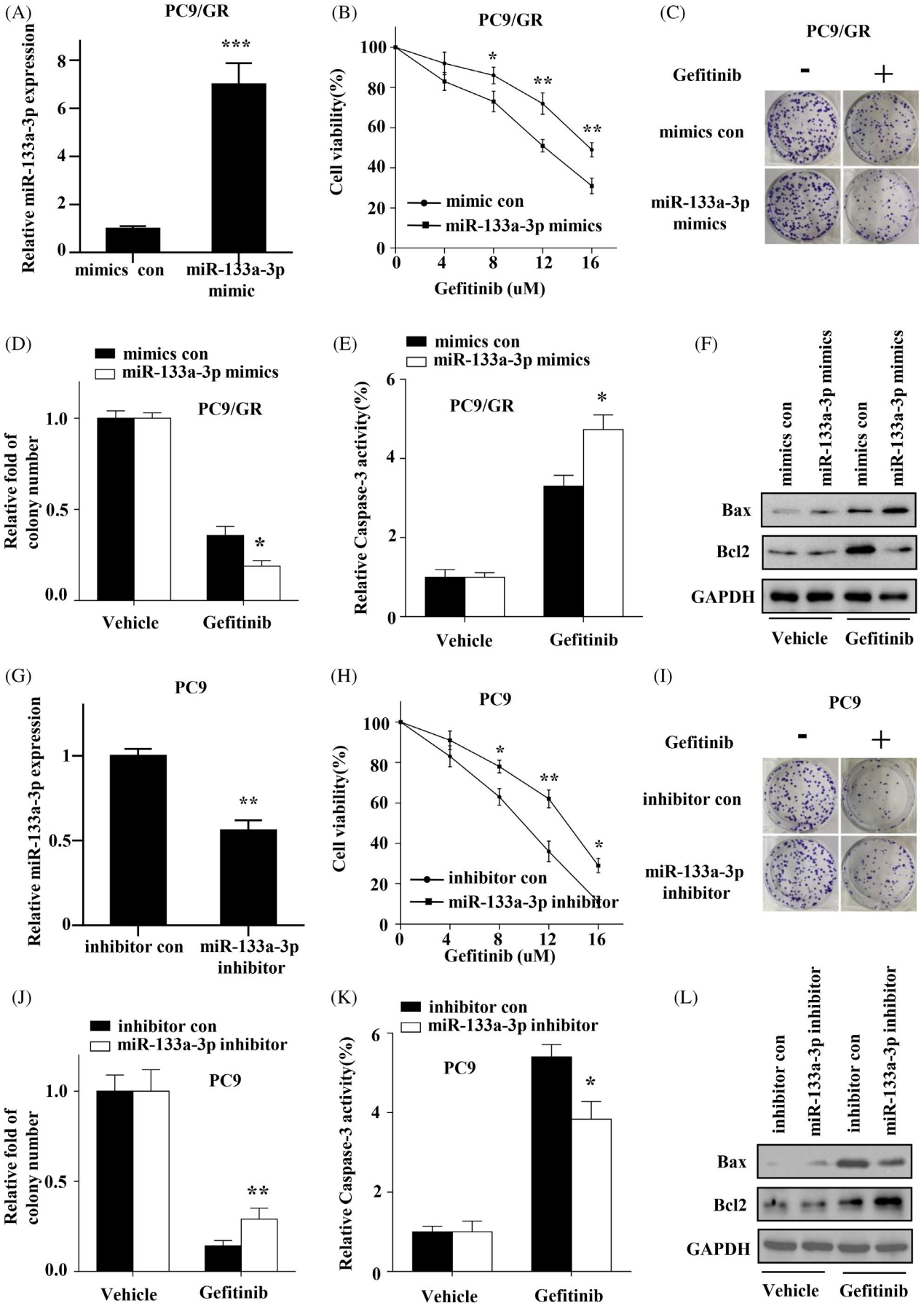
(A)
PC9/GR
Relative miR-133a-3p expression
***
mimics con
miR-133a-3p mimic
(B)
PC9/GR
Cell viability(%)
mimic con
miR-133a-3p mimics
Gefitinib (uM)
(C)
PC9/GR
Gefitinib
mimics con
miR-133a-3p mimics
(D)
mimics con
miR-133a-3p mimics
PC9/GR
Relative fold of colony number
Vehicle
Gefitinib
(E)
mimics con
miR-133a-3p mimics
PC9/GR
Relative Caspase-3 activity(%)
Vehicle
Gefitinib
(F)
mimics con
miR-133a-3p mimics
Bax
Bcl2
GAPDH
Vehicle
Gefitinib
(G)
PC9
Relative miR-133a-3p expression
inhibitor con
miR-133a-3p inhibitor
(H)
PC9
Cell viability(%)
inhibitor con
miR-133a-3p inhibitor
Gefitinib (uM)
(I)
PC9
Gefitinib
inhibitor con
miR-133a-3p inhibitor
(J)
inhibitor con
miR-133a-3p inhibitor
PC9
Relative fold of colony number
Vehicle
Gefitinib
(K)
inhibitor con
miR-133a-3p inhibitor
PC9
Relative Caspase-3 activity(%)
Vehicle
Gefitinib
(L)
inhibitor con
miR-133a-3p inhibitor
Bax
Bcl2
GAPDH
Vehicle
Gefitinib

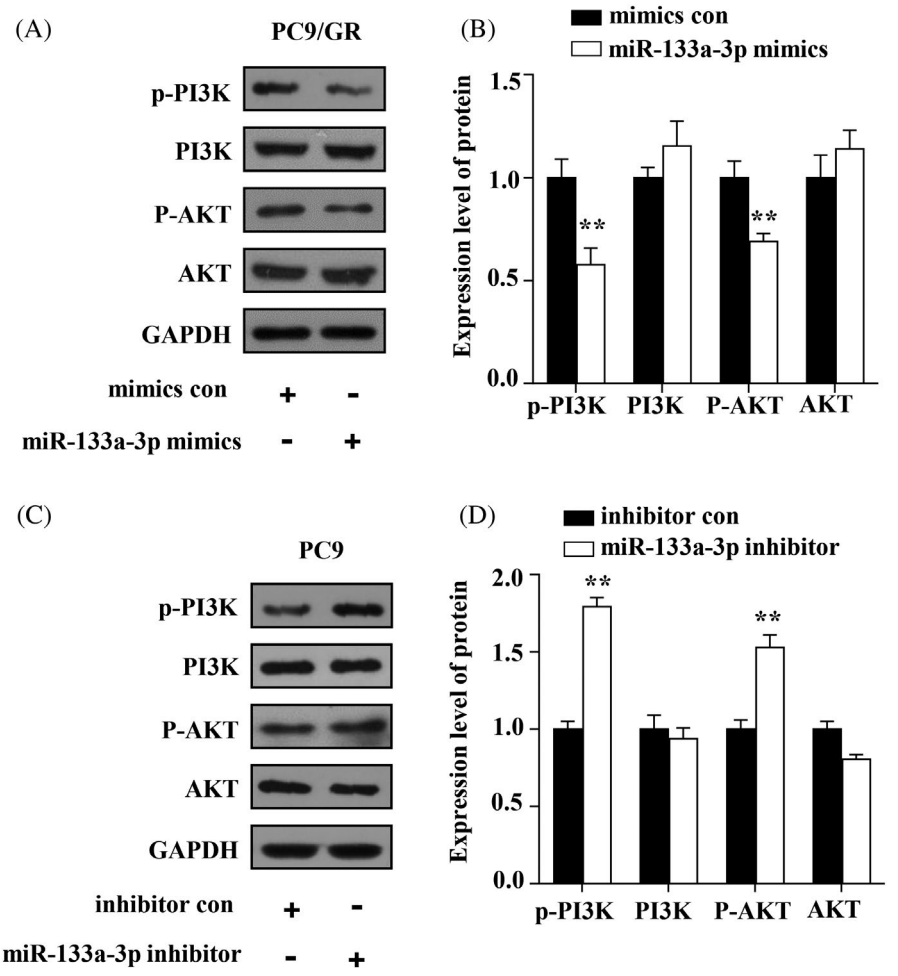

FIGURE 4 miR-133a-3p suppresses PI3K/AKT pathway in PC9/GR cell line. (A) Protein expression of phosphorylated PI3K, total PI3K, phosphorylated AKT, total AKT in PC9/GR cells transfected with miR-133a-3p mimics or mimics control was determined by western blotting. (B) Protein expression of phosphorylated PI3K, total PI3K, phosphorylated AKT, total AKT in PC9 cells transfected with miR-133a-3p inhibitor or inhibitor control was determined by western blotting.

3.6 | miR-133a-3p regulates gefitinib sensitivity in NSCLC cells through targeting SPAG5

To confirm whether SPAG5 plays an important role in the regulation of miR-133a-3p-mediated gefitinib sensitivity in NSCLC cells, a series of rescue experiments were performed. RT-PCR and western blot assays showed that SPAG5 in miR-133a-3p mimic PC9/GR cells transfected with SPAG5 plasmid was overexpressed markedly at both protein and mRNA levels compared with vector plasmid transfection (Figure 6A-B). The results from the CCK-8 assay (Figure 6C), colony-forming assay (Figure 6D), and caspase-3 activity assay (Figure 6E) indicated that overexpression of SPAG5 in miR-133a-3p mimic PC9/GR cells increased the cell proliferation, colony-forming capability, and attenuated cell apoptosis upon to the gefitinib. We also transfected siRNA (si-SPAG5) in miR-133a-3p inhibitor PC9 cells to decrease SPAG5 expression (Figure 6F-G). As expected, decreasing SPAG5 expression in miR-133a-3p inhibitor PC9 cells alleviated gefitinib resistance caused by miR-133a-3p inhibition (Figure 6H-J). Furthermore, western blot demonstrated that SPAG5 overexpression markedly increased p-PI3K and p-AKT expression levels in miR-133a-3p mimic PC9/GR cells (Figure 7A), and SPAG5 low expression significantly decreased p-PI3K and p-AKT expression levels in miR-133a-3p inhibitor PC9 cells (Figure 7B). Taken together, these results suggested that miR-133a-3p regulated gefitinib sensitivity in NSCLC cells through targeting SPAG5.

4 | DISCUSSION

As we all know, gefitinib has effective anti-tumor activity due to its ability to target EGFR to cause the inactivation of downstream signaling pathways and is widely used in the treatment of patients with

FIGURE 5 SPAG5 is a direct target of miR-133a-3p. (A) WT and MUT binding sites for miR-133a-3p in the 3'-UTR of SPAG5. (B) Expression level of miR-133a-3p in LUAD tissues and normal lung tissues in datasets from TCGA database. (C) Expression level of SPAG5 in LUAD tissues and normal lung tissues in datasets from TCGA database. (D) Correlation analysis between miR-133a-3p and SPAG5 expression levels in the tissues of patients with LUAD from TCGA. (E) PC9/GR cells were co-transfected with miR-133a-3p mimics or mimics control and WT- SPAG5 or MUT- SPAG5. Luciferase activity was assessed after 48 h. (F) PC9 cells were co-transfected with miR-133a-3p inhibitor or inhibitor control and WT- SPAG5 or MUT- SPAG5. Luciferase activity was assessed after 48 h. (G-H) SPAG5 mRNA and protein expression in PC9/GR cells transfected with miR-133a-3p mimics or mimics control. (I-J) SPAG5 mRNA and protein expression in PC9 cells transfected with miR-133a-3p inhibitor or inhibitor control.

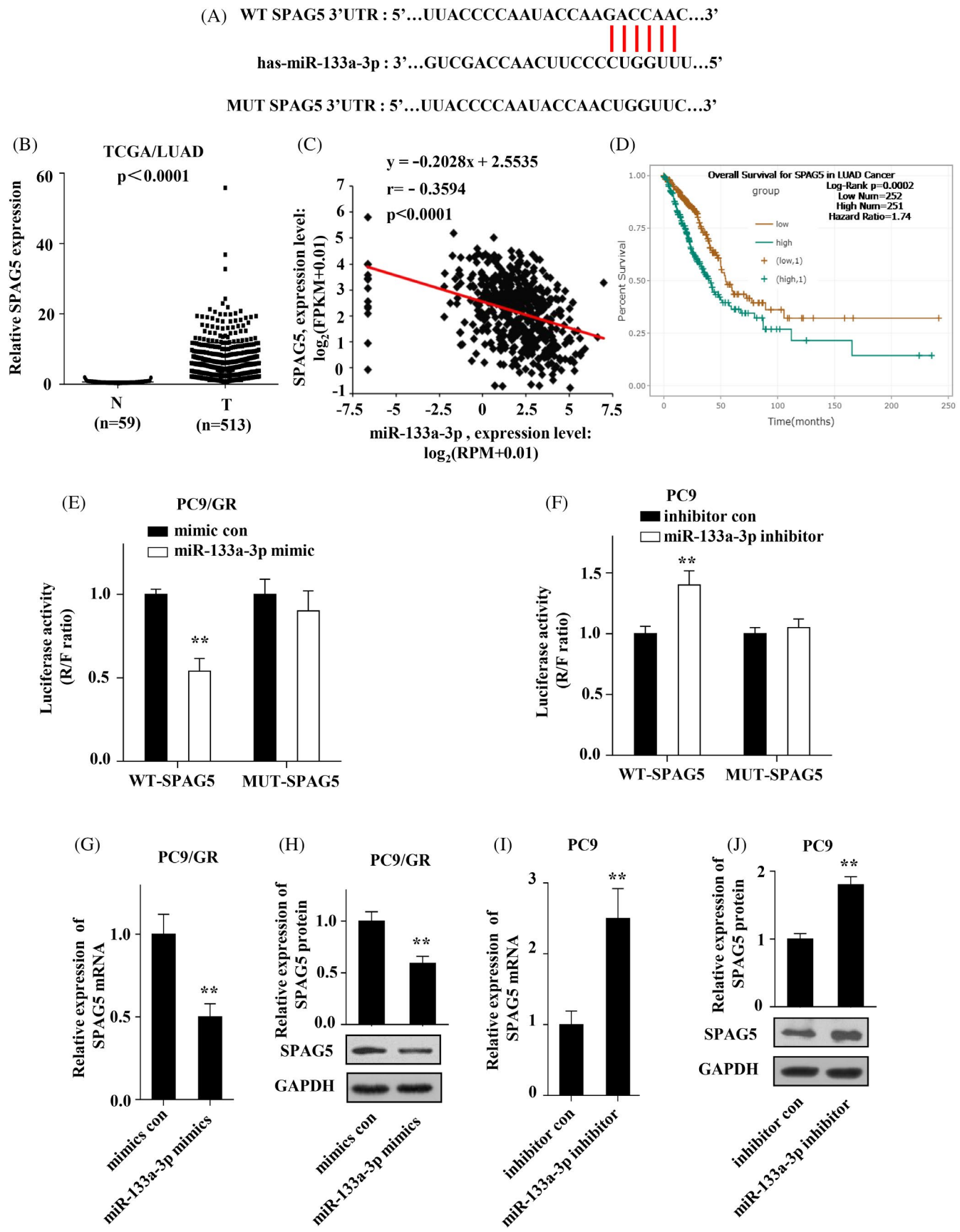
(A)
WT SPAG5 3'UTR : 5'…UUACCCCAAUACCAAGACCAAC…3'
has-miR-133a-3p : 3'…GUCGACCAACUUCCCCUGGUUU…5'
MUT SPAG5 3'UTR : 5'…UUACCCCAAUACCAACUGGUUC…3'
(B)
TCGA/LUAD
p<0.0001
Relative SPAG5 expression
N (n=59)
T (n=513)
(C)
y = -0.2028x + 2.5535
r= - 0.3594
p<0.0001
SPAG5, expression level: log2(FPKM+0.01)
miR-133a-3p , expression level: log2(RPM+0.01)
(D)
Overall Survival for SPAG5 in LUAD Cancer
Log-Rank p=0.0002
Low Num=252
High Num=251
Hazard Ratio=1.74
group
low
high
(low,1)
(high,1)
Percent Survival
Time(months)
(E)
PC9/GR
mimic con
miR-133a-3p mimic
Luciferase activity (R/F ratio)
WT-SPAG5
MUT-SPAG5
(F)
PC9
inhibitor con
miR-133a-3p inhibitor
Luciferase activity (R/F ratio)
WT-SPAG5
MUT-SPAG5
(G)
PC9/GR
Relative expression of SPAG5 mRNA
mimics con
miR-133a-3p mimics
(H)
PC9/GR
Relative expression of SPAG5 protein
SPAG5
GAPDH
mimics con
miR-133a-3p mimics
(I)
PC9
Relative expression of SPAG5 mRNA
inhibitor con
miR-133a-3p inhibitor
(J)
PC9
Relative expression of SPAG5 protein
SPAG5
GAPDH
inhibitor con
miR-133a-3p inhibitor

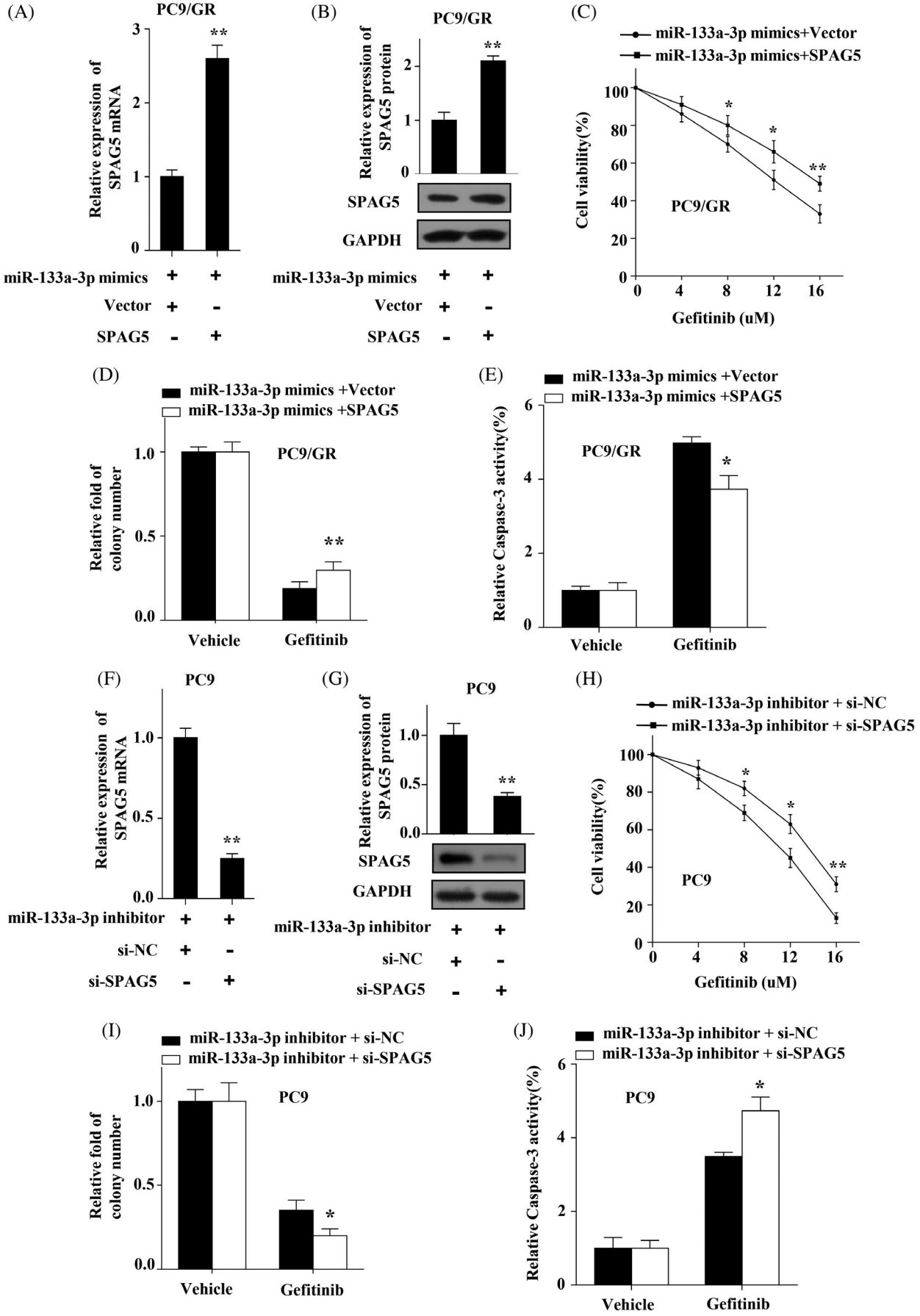
(A)
PC9/GR
Relative expression of SPAG5 mRNA
miR-133a-3p mimics + +
Vector + -
SPAG5 - +
(B)
PC9/GR
Relative expression of SPAG5 protein
SPAG5
GAPDH
miR-133a-3p mimics + +
Vector + -
SPAG5 - +
(C)
miR-133a-3p mimics+Vector
miR-133a-3p mimics+SPAG5
Cell viability(%)
PC9/GR
Gefitinib (uM)
(D)
miR-133a-3p mimics +Vector
miR-133a-3p mimics +SPAG5
Relative fold of colony number
PC9/GR
Vehicle
Gefitinib
(E)
miR-133a-3p mimics +Vector
miR-133a-3p mimics +SPAG5
Relative Caspase-3 activity(%)
PC9/GR
Vehicle
Gefitinib
(F)
PC9
Relative expression of SPAG5 mRNA
miR-133a-3p inhibitor + +
si-NC + -
si-SPAG5 - +
(G)
PC9
Relative expression of SPAG5 protein
SPAG5
GAPDH
miR-133a-3p inhibitor + +
si-NC + -
si-SPAG5 - +
(H)
miR-133a-3p inhibitor + si-NC
miR-133a-3p inhibitor + si-SPAG5
Cell viability(%)
PC9
Gefitinib (uM)
(I)
miR-133a-3p inhibitor + si-NC
miR-133a-3p inhibitor + si-SPAG5
Relative fold of colony number
PC9
Vehicle
Gefitinib
(J)
miR-133a-3p inhibitor + si-NC
miR-133a-3p inhibitor + si-SPAG5
Relative Caspase-3 activity(%)
PC9
Vehicle
Gefitinib

FIGURE 6 miR-133a-3p regulates gefitinib sensitivity in NSCLC cells through targeting SPAG5. (A-B) SPAG5 mRNA and protein expression in PC9/GR cells co-transfected with SPAG5 or vector plasmids and miR-101-3p mimics. (C) Proliferation of PC9/GR cells co-transfected with SPAG5 or vector plasmids and miR-101-3p mimics after treated with various concentrations of gefitinib was determined by CCK8 assay. (D) Colony-forming capability of PC9/GR cells co-transfected with SPAG5 or vector plasmids and miR-101-3p mimics after treated with gefitinib. (E) Caspase-3 activity was detected in cells exposed to gefitinib. (F-G) SPAG5 mRNA and protein expression in PC9 cells co-transfected with si-SPAG5 or si-NC plasmids and miR-101-3p inhibitor. (C) Proliferation of PC9 cells co-transfected with si-SPAG5 or si-NC plasmids and miR-101-3p inhibitor after treated with various concentrations of gefitinib was determined by CCK8 assay. (D) Colony-forming capability of PC9 cells co-transfected with si-SPAG5 or si-NC plasmids and miR-101-3p inhibitor after treated with gefitinib. (E) Caspase-3 activity was detected in cells exposed to gefitinib.

EGFR mutations in NSCLC.[27] However, acquired drug resistance has become an obstacle that hinders gefitinib from exerting its effective anti-tumor activity. Although many studies have described several potential mechanisms of gefitinib resistance, including secondary mutation of EGFR (T790M mutation), overexpression of HGF, MET amplification, and additional genetic alterations,[4] gefitinib resistance still exists. Thus, effective strategies to overcome gefitinib resistance in NSCLC are urgently demanded.

Recently, increasing evidence has shown that miRNAs play an important regulatory role in cancer treatment response and gefitinib resistance.[28] Ge et al[29]. established gefitinib-resistant sub-clone A549 cells and found that transfected miR-7 reversed gefitinib sensitivity in A549 cells. MiR-138-5p enhanced the sensitivity to gefitinib by targeting G protein-coupled receptor124 in PC9/GR cells and H1975 cells.[30] MiRNA-34a inhibited cell growth and induce apoptosis by targeting MET in hepatocyte growth factor (HGF)-induced gefitinib-resistant HCC827 and PC9 cells.[31] In this study, we successfully established a gefitinib-resistant cell line (PC9/GR) and found that miR-133a-3p was significantly downregulated in the gefitinib-resistant cell line PC9/GR compared with gefitinib-sensitive cell line PC9. Previously, miR-133a-3p has been reported to be downregulated in many cancers, and low expression of miR-133a-3p was associated with tumor recurrence, metastasis, drug resistance, and poor prognosis of cancer patients.[32-34] Our results also indicate that low expression of miR-133a-3p in lung cancer tissues is associated with poor prognosis in patients with lung cancer. Thus, we hypothesized that the downregulation of miR-133a-3p expression may support the gefitinib resistance in PC9/GR cells. As expected, the results from the CCK8 assay, colony formation assay, caspase-3 activity assay indicated that upregulation of miR-133a-3p expression decreased gefitinib resistance of PC9/GR cells. In turn, downregulation of miR-133a-3p expression increased the gefitinib

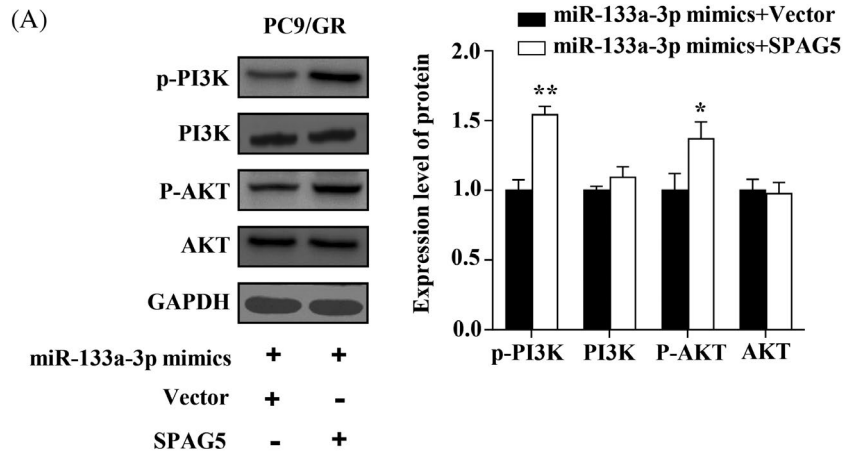

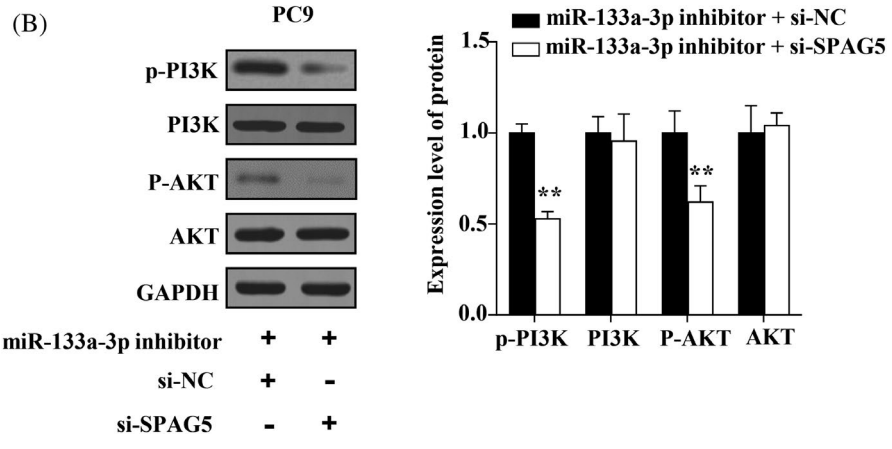

FIGURE 7 SPAG5 reverses miR-133a-3p-inactivated PI3K/AKT pathway in PC9/GR cell. (A) Protein expression of phosphorylated PI3K, total PI3K, phosphorylated AKT, total AKT in PC9/GR cells co-transfected with SPAG5 or vector plasmids and miR-101-3p mimics was determined by western blotting. (B) Protein expression of phosphorylated PI3K, total PI3K, phosphorylated AKT, total AKT in PC9 cells co-transfected with si-SPAG5 or si-NC plasmids and miR-101-3p inhibitor was determined by western blotting.

resistance of PC9 cells. These results indicated that miR-133a-3p may play an important role in regulating the gefitinib sensitivity of NSCLC patients.

Activation of the PI3K/AKT pathway is frequently implicated in resistance to anticancer therapies including targeted therapy with gefitinib.[35] And inhibitors of PI3K/AKT pathway, such as PI3K inhibitor, could restore therapeutic sensitivity of tumors that have acquired resistance to standard therapy.[36] Thus, inhibitors of PI3K/AKT pathway in combination with gefitinib have great potential in the treatment of NSCLC patients with acquired gefitinib resistance. In this study, we found that upregulation of miR-133a-3p expression decreased p-PI3K and p-AKT expression levels in PC9/GR cells, and in turn, downregulation of miR-133a-3p expression increased p-PI3K and p-AKT expression level in PC9 cells. This suggested that miR-133a-3p may be a potential inhibitor of PI3K/AKT pathway, and activation of the PI3K/AKT pathway due to the low expression of miR-133a-3p was an important cause of gefitinib resistance.

Further, we predicted the target of miR-133a-3p to better understand the mechanism of gefitinib resistance. SPAG5 was selected as a potential candidate target gene of miR-133a-3p. SPAG5 has been reported to be overexpressed in a variety of cancers including NSCLC and is closely linked to tumor progression, drug resistance, and poor prognosis of cancer patients.[18,19] Recently, Yang *et al*. confirmed that the highly expressed SPAG5 can activate the PI3K/AKT signaling pathway in hepatocellular carcinoma.[20] Thus, we hypothesized SPAG5 was a direct target of miR-133a-3p in the regulation of the PI3K/AKT signaling pathway. To prove our hypothesis, we first observed a significant negative expression correlation between miR-133a-3p and SPAG5 in NSCLC patient tissues. The dual-luciferase reporter assay indicated that miR-133a-3p can indeed directly bind to 3'-UTR of SPAG5. The inhibitory effect of miR-133a-3p on SPAG5 expression was further verified in PC9/GR and PC9 cells.

To further clarify that miR-133a-3p regulates gefitinib sensitivity and PI3K/AKT signaling pathway in NSCLC cells through targeting SPAG5, we performed a series of rescue experiments and found that upregulation of SPAG5 did reverse miR-133a-3p-increased gefitinib sensitivity and inactivated PI3K/AKT signaling pathway in PC/GR cells, and downregulation of SPAG5 also reverse gefitinib resistance caused by the inhibition of miR-133a-3p in PC9 cells. Those results indicated that SPAG5 had a key role in miR-133a-3p-mediated gefitinib sensitivity and PI3K/AKT signaling inactivation.

However, there are some limitations in this study. We found that the expression of miR-133a-3p was significantly reduced in the constructed drug-resistant PC9 cell lines, but further verification of clinical samples and other data is still needed. In our study, NSCLC patients with low expression of miR-133a-3p have a poor prognosis, but clinical data are still needed to confirm whether miR-133a-3p affects the prognosis of patients following treatment with gefitinib.

In summary, our findings suggested that miR-133a-3p could reverse gefitinib resistance in NSCLC cells by targeting SPAG5. Therefore, miR-133a-3p/SPAGE5 axis might become a novel strategy in treating gefitinib-resistance NSCLC.

ACKNOWLEDGEMENTS

None.

CONFLICT OF INTEREST

The authors declare no conflicts of interest.

DATA AVAILABILITY STATEMENT

All data are included in this article.

ORCID

Qing Li https://orcid.org/0000-0002-3023-0419

REFERENCES

1. Torre LA, Bray F, Siegel RL, Ferlay J, Lortet-Tieulent J, Jemal A. Global cancer statistics, 2012. *CA Cancer J Clin*. 2015;65(2):87-108.
2. Schiller JH, Harrington D, Belani CP, et al. Comparison of four chemotherapy regimens for advanced non-small-cell lung cancer. *N Engl J Med*. 2002;346(2):92-98.
3. Herbst RS, Fukuoka M, Baselga J. Gefitinib–a novel targeted approach to treating cancer. *Nat Rev Cancer*. 2004;4(12):956-965.
4. Remon J, Morán T, Majem M, et al. Acquired resistance to epidermal growth factor receptor tyrosine kinase inhibitors in EGFR-mutant non-small cell lung cancer: a new era begins. *Cancer Treat Rev*. 2014;40(1):93-101.
5. Bartel DP. MicroRNAs: genomics, biogenesis, mechanism, and function. *Cell*. 2004;116(2):281-297.
6. Lin S, Gregory RI. MicroRNA biogenesis pathways in cancer. *Nat Rev Cancer*. 2015;15(6):321-333.
7. Piletič K, Kunej T. MicroRNA epigenetic signatures in human disease. *Arch Toxicol*. 2016;90(10):2405-2419.
8. Calin GA, Croce CM. MicroRNA signatures in human cancers. *Nat Rev Cancer*. 2006;6(11):857-866.
9. Shi W, Tang T, Li X, et al. Methylation-mediated silencing of miR-133a-3p promotes breast cancer cell migration and stemness via miR-133a-3p/MAML1/DNMT3A positive feedback loop. *J Exp Clin Cancer Res: CR*. 2019;38(1):429.
10. Yin Y, Du L, Li X, Zhang X, Gao Y. miR-133a-3p suppresses cell proliferation, migration, and invasion and promotes apoptosis in esophageal squamous cell carcinoma. *J Cell Physiol*. 2019;234(8):12757-12770.
11. Han S, Ding X, Wang S. miR-133a-3p Regulates Hepatocellular Carcinoma Progression Through Targeting CORO1C. *Cancer Manag Res*. 2020;12:8685-8693.
12. Xu Y, Zhang L, Xia L, Zhu X. MicroRNA-133a-3p suppresses malignant behavior of non-small cell lung cancer cells by negatively regulating ERBB2. *Oncol Lett*. 2021;21(6):457.
13. Wang X, Zhu W, Zhao X, Wang P. miR-133a enhances the sensitivity of Hep-2 cells and vincristine-resistant Hep-2v cells to cisplatin by downregulating ATP7B expression. *Int J Mol Med*. 2016;37(6):1636-1642.
14. Yuan Y, Yao YF, Hu SN, Gao J, Zhang LL. MiR-133a Is Functionally Involved in Doxorubicin-Resistance in Breast Cancer Cells MCF-7 via Its Regulation of the Expression of Uncoupling Protein 2. *PLoS One*. 2015;10(6):e0129843.
15. Thein KH, Kleylein-Sohn J, Nigg EA, Gruneberg U. Astrin is required for the maintenance of sister chromatid cohesion and centrosome integrity. *J Cell Biol*. 2007;178(3):345-354.
16. Chang MS, Huang CJ, Chen ML, et al. Cloning and characterization of hMAP126, a new member of mitotic spindle-associated proteins. *Biochem Biophys Res Comm*. 2001;287(1):116-121.
17. He J, Green AR, Li Y, Chan SYT, Liu DX. SPAG5: an emerging oncogene. *Trends Cancer*. 2020;6(7):543-547.

18. Li M, Li A, Zhou S, Lv H, Yang W. SPAG5 upregulation contributes to enhanced c-MYC transcriptional activity via interaction with c-MYC binding protein in triple-negative breast cancer. *J Hematol Oncol*. 2019;12(1):14.
19. Wang T, Li K, Song H, et al. p53 suppression is essential for oncogenic SPAG5 upregulation in lung adenocarcinoma. *Biochem Biophys Res Comm*. 2019;513(2):319-325.
20. Yang YF, Zhang MF, Tian QH, et al. SPAG5 interacts with CEP55 and exerts oncogenic activities via PI3K/AKT pathway in hepatocellular carcinoma. *Mol Cancer*. 2018;17(1):117.
21. Zhang H, Li S, Yang X, Qiao B, Zhang Z, Xu Y. miR-539 inhibits prostate cancer progression by directly targeting SPAG5. *J Exp Clin Cancer Res : CR*. 2016;35:60.
22. Abdel-Fatah TMA, Agarwal D, Liu DX, et al. SPAG5 as a prognostic biomarker and chemotherapy sensitivity predictor in breast cancer: a retrospective, integrated genomic, transcriptomic, and protein analysis. *Lancet Oncol*. 2016;17(7):1004-1018.
23. Yuan LJ, Li JD, Zhang L, et al. SPAG5 upregulation predicts poor prognosis in cervical cancer patients and alters sensitivity to taxol treatment via the mTOR signaling pathway. *Cell Death Dis*. 2014;5(5):e1247.
24. Yang JH, Li JH, Shao P, Zhou H, Chen YQ, Qu LH. starBase: a database for exploring microRNA–mRNA interaction maps from Argonaute CLIP-Seq and Degradome-Seq data. *Nucleic Acids Res*. 2011;39(suppl_1):D202-D209.
25. Yamamoto C, Basaki Y, Kawahara A, et al. Loss of PTEN expression by blocking nuclear translocation of EGR1 in gefitinib-resistant lung cancer cells harboring epidermal growth factor receptor-activating mutations. *Can Res*. 2010;70(21):8715-8725.
26. Shien K, Ueno T, Tsukuda K, et al. Knockdown of the epidermal growth factor receptor gene to investigate its therapeutic potential for the treatment of non-small-cell lung cancers. *Clin Lung Cancer*. 2012;13(6):488-493.
27. Herbst RS. Review of epidermal growth factor receptor biology. *Int J Radiat Oncol Biol Phys*. 2004;59(2 Suppl):21-26.
28. Wu Q, Yang Z, Shi Y, Fan D. MiRNAs in human cancers: the diagnostic and therapeutic implications. *Curr Pharm Des*. 2014;20(33):5336-5347.
29. Ge X, Zheng L, Huang M, Wang Y, Bi F. MicroRNA expression profiles associated with acquired gefitinib-resistance in human lung adenocarcinoma cells. *Mol Med Rep*. 2015;11(1):333-340.
30. Gao Y, Fan X, Li W, Ping W, Deng Y, Fu X. miR-138-5p reverses gefitinib resistance in non-small cell lung cancer cells via negatively regulating G protein-coupled receptor 124. *Biochem Biophys Res Comm*. 2014;446(1):179-186.
31. Zhou JY, Chen X, Zhao J, et al. MicroRNA-34a overcomes HGF-mediated gefitinib resistance in EGFR mutant lung cancer cells partly by targeting MET. *Cancer Lett*. 2014;351(2):265-271.
32. Tang Y, Pan J, Huang S, et al. Downregulation of miR-133a-3p promotes prostate cancer bone metastasis via activating PI3K/AKT signaling. *J Exp Clin Cancer Res: CR*. 2018;37(1):160.
33. Liang Z, Liu Z, Cheng C, et al. VPS33B interacts with NESG1 to modulate EGFR/PI3K/AKT/c-Myc/P53/miR-133a-3p signaling and induce 5-fluorouracil sensitivity in nasopharyngeal carcinoma. *Cell Death Dis*. 2019;10(4):305.
34. Bitaraf A, Babashah S, Garshasbi M. Aberrant expression of a five-microRNA signature in breast carcinoma as a promising biomarker for diagnosis. *J Clin Lab Anal*. 2020;34(2):e23063.
35. Burris HA 3rd. Overcoming acquired resistance to anticancer therapy: focus on the PI3K/AKT/mTOR pathway. *Cancer Chemother Pharmacol*. 2013;71(4):829-842.
36. Papadimitrakopoulou V. Development of PI3K/AKT/mTOR pathway inhibitors and their application in personalized therapy for non-small-cell lung cancer. *J Thorac Oncol*. 2012;7(8):1315-1326.

How to cite this article: Li Q, Wang Y, He J. MiR-133a-3p attenuates resistance of non-small cell lung cancer cells to gefitinib by targeting SPAG5. *J Clin Lab Anal*. 2021;35:e23853. https://doi.org/10.1002/jcla.23853